Applied Physics A (2023) 129:304
https://doi.org/10.1007/s00339-023-06523-2

Applied Physics A
Materials Science & Processing

Giant cross-Kerr nonlinearity in the metal nanoparticles-graphene nanodisks-quantum dots hybrid system with low light intensity for photovoltaic devices

Mariam M. Tohari[1] · Moteb Alqahtani[1] · Ghadah M. Almzargah[1]

Received: 13 September 2022 / Accepted: 22 February 2023 / Published online: 31 March 2023

Abstract
The ability of plasmonics nanostructures to enhance light-matter interaction due to trapping and localizing the light at the nanoscale make them an efficient platform for energy conversion devices. In the present paper, we theoretically study cross-Kerr nonlinear absorption of the metal nanoparticles-graphene nanodisks-quantum dots hybrid plasmonic system under the weak-field approximation. We obtain a giant cross-Kerr nonlinearity resulting in large nonlinear absorption coefficients in the visible region of the electromagnetic spectrum with low light intensity. We find that the cross-Kerr nonlinear optical properties of the system can be controlled in magnitude and sign by the geometrical parameters of the system and interacting fields. The system exhibits good stability with this nonlinear behavior providing a promising platform for many optical devices including energy conversion devices.

Keywords Cross-Kerr nonlinearity · Nonlinear absorption coefficient · Metal nanoparticles-graphene nanodisks-quantum dots hybrid system · Photovoltaic devices

1 Introduction

Nonlinear materials have stimulated much interest due to their important role in the development of modern photonics and optoelectronics [1]. Thus, much effort has been devoted to understanding the nonlinear polarization mechanisms and their relation to the structural characteristics of nonlinear materials [2]. Intense light fields are indeed required to manipulate the optical properties of materials and induce nonlinear phenomena. The effective nonlinear optical response can fortunately be induced with low light intensity through interaction with plasmonic materials [3–6]. Specifically, when the light fields interact with the free electrons on the surface of metals, they induce collective oscillations called surface plasmons resulting in strong local electromagnetic fields that can enhance the nonlinearity of the plasmonic systems [7]. Moreover, nanoplasmonics enable strong light-matter interaction with a high density of states that can lead to additional efficiency of energy conversion [8, 9]. Interestingly, controlling the optical properties of the hybrid nanoplasmonic systems, where the energy can transfer between the components of the systems, [10–16] provides a promising platform for energy conversion devices such as photovoltaic devices [17–22].

In photovoltaic devices, maximizing absorption is desirable to create additional electron–hole pairs that initiate generation with appreciable efficiency. The nonlinear optical properties relate to higher efficiency of mobility and electron transport from donor to acceptor. Due to the ability of plasmonics to induce nonlinearity with low light intensity, some undesirable nonlinear processes that reduce the energy conversion efficiency such as two-photon absorption can be avoided [23]. It has been shown that the materials of high third-order nonlinearity with low light intensity can be employed in solar cell applications [24, 25]. Therefore, plasmonic nanocompositions, where

Moteb Alqahtani and Ghadah M. Almzargah have equally contributed to this work.

✉ Mariam M. Tohari
mrohary@kku.edu.sa

Moteb Alqahtani
moalqahtani@kku.edu.sa

Ghadah M. Almzargah
ghadahalmzargah@gmail.com

[1] Department of Physics, King Khalid University, Abha 9004, Asir, Saudi Arabia

electromagnetic fields experience a large enhancement even with low light intensity and exhibit a large third-order nonlinearity within a tunable spectral region controlled by the size and dielectric properties of these materials, can be used to build efficient devices for energy conversion [5, 26–28]. The enhanced nonlinear absorption of radiation in the visible and near-infrared regions with good stability is an essential parameter that can be used to measure the efficiency of solar cells.

It has been found that cross-Kerr nonlinearity describing cross-coupling effects is twice as large as that of self-action effects [29]. More precisely, the cross-Kerr nonlinearity describes the change in refractive index experienced by an electric field propagating in the Kerr medium and controlled by another applied field. Because the significant potential applications of cross-Kerr nonlinearity in optical devices [30–32], several schemes have been theoretically and experimentally studied to control this type of nonlinearity and suggest suitable applications. [33–42]. In most cases, the large Kerr nonlinearity with a changeable sign is often needed to gain conversion efficiency [43]. Thus, cross-Kerr nonlinearity has been examined for some plasmonic systems. H. Rhman et al. have examined cross-Kerr nonlinearity in surface plasmon waves generated at the interface between graphene and gain medium [44]. It has been shown that the propagation length of the surface plasmons can be significantly controlled under Kerr nonlinearity and strength of the control fields. Moreover, high cross nonlinear refractive index has been observed in a five-level quantum system near plasmonic nanostructure via probe field amplification [45].

Interestingly, taking advantage of high mobility and the long propagation distances of the charge carriers in the graphene, in addition to the high charge density in a metal as well as the relatively low decay rate and localized charges in quantum dots which can induce atomic coherence if they are modeled as muli-level atomic systems, graphene nanodisks-metal nanoparticles-quantum dots (GNDs-MNPs-QDs) hybrid plasmonic system has been proposed by M. Tohari et al. which demonstrates ultrafast dynamics [46] and a giant self-Kerr nonlinearity [5] in the visible region of the electromagnetic spectrum with low light intensity can be controlled in magnitude and sign by the parameters of the system enabling various interesting potential applications in photonics and optoelectronics.

Motivated by the high nonlinearity that has been recently shown in our proposed hybrid plasmonic system [5, 47, 48], we analytically investigate in the present paper the nonlinear absorption coefficient of the system experienced by the probe field due to another applied control field resulting in the cross-Kerr effect. The probe field is adjusted to be resonant with surface plasmons of visible energy that matches the gain energy of the quantum dots. The metal nanoparticle that has the ability to control the optical properties of the adjacent graphene nanodisk is also inserted in the system.

The paper is organized as follows: in "Theoretical model" the model is established by describing the relevant mathematical techniques and the physical assumptions. Section "Results and discussion" displays the numerical simulations and discusses the analytical results of cross-Kerr nonlinearity of the system and "Conclusions" summarizes the main conclusions.

2 Theoretical model

Suppose a hybrid plasmonic system depicted in Fig. 1 consisting of GND of radius L_z and thickness L_x doped at Fermi energy E_F with mobility of μ for charge carriers. The GND is placed at a distance R_{GQ} from the quantum dot modeled as a three -level atomic system of Λ configuration. Additionally, a MNP is inserted within the system at distances R_{GM} and R_{QM} from the GND and QD respectively. The QD of a three-level atomic system of Λ configuration interacts with two applied fields, probe and control fields. Due to the unique properties of graphene charge carriers, the surface plasmons of GND is set to be resonant with the excitons of QD.The MNP is incorporated in the system to control the optical properties of the GND [46]. The probe field E_P is monitored to be resonant with surface plasmons of GND at the visible region of the electromagnetic spectrum inducing the transition $|1\rangle \longleftrightarrow |2\rangle$ with dipole moment μ_{12} and decay rate γ_{12}. On the other hand, the transition $|1\rangle \longleftrightarrow |3\rangle$ is mediated by the control field E_c with dipole moment μ_{13} and decay rate γ_{13}.

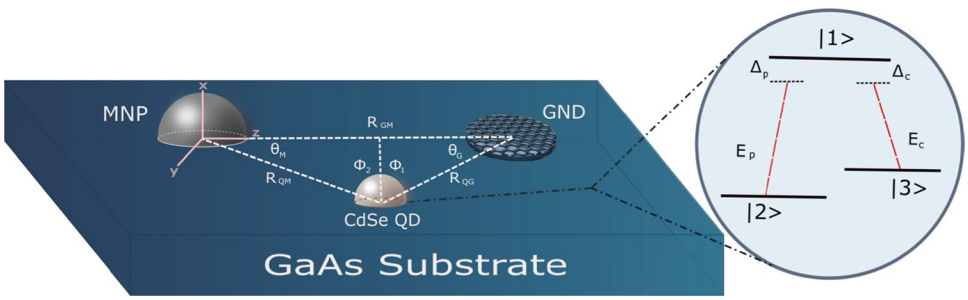

Fig. 1 The MNP–GND–QD hybrid system setup

Analyzing the dipole-dipole interaction between the components of the system, one can use the corresponding interaction Hamiltonian given in terms of the dipole field felt by the QD to obtain the following equation of motion for the matrix elements of the density operators that describe the dynamics of the system [46]:

$$\dot{\rho}_{13} = -\left[\left(\frac{\gamma_{13}}{2}+\frac{\gamma_{12}}{2}\right)+i\left(\Delta_c-\Lambda_z\left(\rho_{33}-\rho_{11}\right)\right)\right]\rho_{13} + i\Omega_c\left(\Pi_z+\Phi_z\right)\left(\rho_{33}-\rho_{11}\right)+i\left[\Omega_p\left(\Pi_x+\Phi_x\right)+\Lambda_x\rho_{12}\right]\rho_{23}, \tag{1a}$$

$$\dot{\rho}_{12} = -\left[\left(\frac{\gamma_{13}}{2}+\frac{\gamma_{12}}{2}\right)+i\left(\Delta_p-\Lambda_x\left(\rho_{22}-\rho_{11}\right)\right)\right]\rho_{12} + i\Omega_p\left(\Pi_x+\Phi_x\right)\left(\rho_{22}-\rho_{11}\right)+i\left[\Omega_c\left(\Pi_z+\Phi_z\right)+\Lambda_z\rho_{13}\right]\rho_{32}, \tag{1b}$$

$$\dot{\rho}_{32} = -\left(\frac{\gamma_{32}}{2}+i\Delta_2\right)\rho_{32}+i\left[\Omega_c^*\left(\Pi_z^*+\Phi_z^*\right)+\Lambda_z^*\rho_{31}\right]\rho_{12} - i\left[\Omega_p\left(\Pi_x+\Phi_x\right)+\Lambda_x\rho_{12}\right]\rho_{31}, \tag{1c}$$

$$\dot{\rho}_{11} = -\left(\gamma_{12}+\gamma_{13}\right)\rho_{11}+i\left[\Omega_c\left(\Pi_z+\Phi_z\right)+\Lambda_z\rho_{13}\right]\rho_{31} + i\left[\Omega_p\left(\Pi_x+\Phi_x\right)+\Lambda_x\rho_{12}\right]\rho_{21}+c.c., \tag{1d}$$

$$\dot{\rho}_{22} = \gamma_{12}\rho_{11}+\gamma_{32}\rho_{33}-i\left[\Omega_p\left(\Pi_x+\Phi_x\right)+\Lambda_x\rho_{12}\right]\rho_{21}+c.c., \tag{1e}$$

$$\dot{\rho}_{33} = \gamma_{13}\rho_{11}-\gamma_{32}\rho_{33}-i\left[\Omega_c\left(\Pi_z+\Phi_z\right)+\Lambda_z\rho_{13}\right]\rho_{31}+c.c. \tag{1f}$$

where $\Pi_{x,z}$, $\Phi_{x,z}$ and $\Lambda_{x,z}$ are the dipole-dipole interaction factors that are given in terms of the geometrical features of the system as [46]:

$$\Pi_x = \frac{1}{4\pi\epsilon^*}\left[\frac{\alpha_G^x\left(3\cos\phi_1-1\right)}{R_{QG}^3}+\frac{\alpha_M\left(3\cos\phi_2-1\right)}{R_{QM}^3}\right], \tag{2a}$$

$$\Lambda_x = \frac{\mu_{12}^2}{(4\pi\epsilon^*)^2\hbar\epsilon_0\epsilon_b}\left[\frac{\alpha_G^x\left(3\cos\phi_1-1\right)^2}{R_{QG}^6}+\frac{\alpha_M\left(3\cos\phi_2-1\right)^2}{R_{QM}^6}\right], \tag{2b}$$

$$\Phi_x = \frac{-\alpha_G^x\alpha_M}{(4\pi\epsilon^*)^2R_{GM}^3}\left[\frac{3\cos\phi_1-1}{R_{QG}^3}+\frac{3\cos\phi_2-1}{R_{QM}^3}\right], \tag{2c}$$

$$\Pi_z = \frac{1}{4\pi\epsilon^*}\left[\frac{\alpha_G^z\left(3\cos\theta_G-1\right)}{R_{QG}^3}+\frac{\alpha_M\left(3\cos\theta_M-1\right)}{R_{QM}^3}\right], \tag{2d}$$

$$\Lambda_z = \frac{\mu_{13}^2}{(4\pi\epsilon^*)^2\hbar\epsilon_0\epsilon_b}\left[\frac{\alpha_G^z\left(3\cos\theta_G-1\right)^2}{R_{QG}^6}+\frac{\alpha_M\left(3\cos\theta_M-1\right)^2}{R_{QM}^6}\right], \tag{2e}$$

$$\Phi_z = \frac{2\alpha_G^z\alpha_M}{(4\pi\epsilon^*)^2R_{GM}^3}\left[\frac{3\cos\theta_G-1}{R_{QG}^3}+\frac{3\cos\theta_M-1}{R_{QM}^3}\right]. \tag{2f}$$

α_G^x (α_G^z) is the shape-dependent polarizability of GND induced by x-polarized (z-polarized) light given in terms of the dimensions of GND, depolarization factors resulting from the asymmetry of GND [46], the dielectric constants of GND and the surrounding medium. $\epsilon^* = (2\epsilon_b-\epsilon_q)/3\epsilon_b$ is the effective dielectric constant, where ϵ_b and ϵ_q are the dielectric constants of background and the QD respectively. Similarly, α_M is the shape-dependent polarizability of MNP given in terms of its dimensions and the dielectric constants of MNP and the surrounding medium. Remarkably, the angles and distances between the components of the system are governed by the triangle law.

$$\chi = \frac{2iNd_{12}}{\epsilon_0E_p}\frac{\Omega_p\left(\Pi_x+\Phi_x\right)}{F}\times\left[\left(1-\frac{2\gamma_{32}}{2\gamma+\gamma_{12}}\right) -\frac{4\Omega_p^2|\Pi_x+\Phi_x|^2}{2\gamma+\gamma_{12}}\left(\frac{1}{F}+\frac{1}{F^*}+\frac{i(\Lambda_x-\Lambda_x^*)}{|F|^2}\right)\right] \tag{3}$$

Using an iterative technique, where the density matrix element can be written as $\rho_{nm} = \rho_{nm}^{(0)}+\rho_{nm}^{(1)}+\rho_{nm}^{(2)}+\cdots$, and at steady state under the weak probe field approximation where the control field is much stronger than the probe field, i.e. $\rho_{11}^{(0)} = 0$ and $\rho_{22}^{(0)} = 1$, M. Tohari et al. have found that the total susceptibility of the system can be given as [5]: To study the nonlinearity of the system resulting from the cross-Kerr effect due to the applied control field, we need to write the total susceptibility of the system in terms of control field i.e., $\chi = \chi^{(1)}+3\chi^{(3)}E_c^2$. This requires to make the Taylor expansion over Ω_c to eventually obtain:

$$\chi^{(1)} = A \times \left[\frac{1}{B}\left(1 - \frac{2\gamma_{32}}{2\gamma + \gamma_{12}}\right) - 4\Omega_p^2 \frac{\Pi_x + \Phi_x}{2\gamma + \gamma_{12}}\left(\frac{1}{B^2} + \frac{1}{B^2} + i\frac{\Lambda_x - \Lambda_x^*}{B^2 + B^*}\right)\right] \tag{4}$$

$$\chi^{(3)} = A\left(\frac{C}{B^2}\right)\left(1 - \frac{2\gamma_{32}}{2\gamma + \gamma_{12}}\right) - A\left(\frac{4|\Pi_x + \Phi_x|^2}{2\gamma + \gamma_{12}}\right) \left[\frac{2C}{B^3} + \frac{C}{B^* B^2} + \frac{C^*}{B^{*2} B} + (\Lambda_x - \Lambda_x^*)\left(\frac{2C}{B^* B^3} + \frac{C^*}{B^{*2} B^*}\right)\right] \tag{5}$$

where

$$A = \frac{-4iN\mu_{12}\mu_{13}^2}{3\epsilon_0 \hbar^2 E_p}(\Pi_x + \Phi_x)\Omega_p \tag{6}$$

$$B = \left(\frac{\gamma_{12}}{2} + \frac{\gamma_{13}}{2}\right) + i(\Delta_p - \Lambda_x) \tag{7}$$

$$C = \frac{|\Pi_z + \Phi_z|^2}{\gamma_{32}/2 + i\Delta_2} \tag{8}$$

In terms of third-order nonlinear susceptibility that describes the cross-Kerr effect, cross Kerr nonlinear refractive index n_2 and the corresponding nonlinear absorption coefficient β are [29]:

$$n_2 = \frac{3Re\left[\chi^{(3)}\right]}{2\epsilon_0 c n_0^2} \quad \text{and} \quad n_0 = \sqrt{1 + Re\left[\chi^{(1)}\right]} \tag{9a}$$

$$\beta = \frac{\omega}{\epsilon_0 c^2 n_0^2} Im\left[\chi^{(3)}\right] \tag{9b}$$

3 Results and discussion

In this section we illustrate the analytical results for the nonlinear absorption coefficient for the hybrid plasmonic system depicted in Fig. 1. Specifically, for a monolayer GND of thickness $L_x = 0.35$ nm and radius $L_z = 7$ nm [49], doped

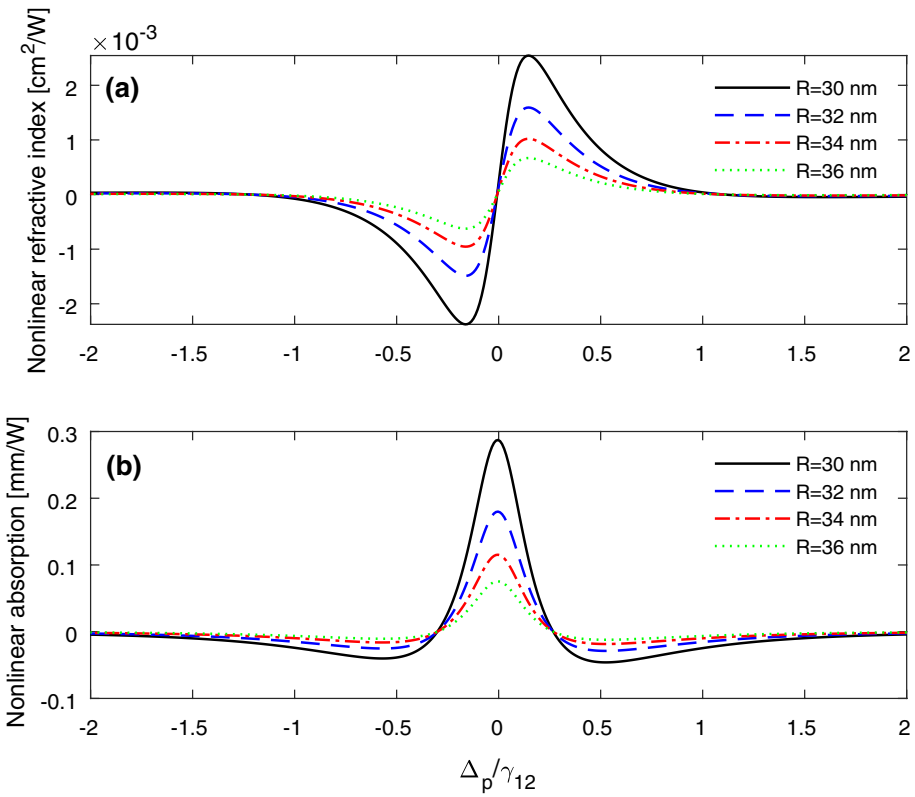

Fig. 2 Cross-Kerr nonlinearity versus probe field detuning of the MNP-GND-QD hybrid system of geometry $\theta_M = \theta_G = 1$ rad, $R_M = 15$ nm, for different values of R. The system interacts with the resonant control field of $\Omega_c = 1\,\mathrm{MH_Z}$ and the probe field of $\Omega_p = 0.01\Omega_c$

at level $E_F = 1.36\,\mathrm{e\,V}$ and has charge carriers of mobility $\mu = 10^4\,\mathrm{cm^2V^{-1}s^{-1}}$ embedded in a GaAs background. For these parameters, two plasmonic resonances can be induced by x and z polarized light fields, $\hbar\omega_{sp}^{x} = 2.1724\,\mathrm{e\,V}$ and $\hbar\omega_{sp}^{z} = 0.6418\,\mathrm{e\,V}$ [5]. Since we aim to study the efficiency of the present system as a photovoltaic device, we choose the visible resonance $\hbar\omega_{sp}^{x} = 2.1724\,\mathrm{e\,V}$ which matches the exciton energy of CdSe QD of atomic density $N = 10^{20}\mathrm{m}^{-3}$ modelled as a three-level atomic system of Λ configuration as illustrated in Fig. 1 [5]. The parameters of the QD are set to be $\mu_{12} = \mu_{13} = 1\mathrm{enm}$, $\gamma_{12} = \gamma_{13} = 1\,\mathrm{GH_Z}$ and $\gamma_{32} = 0.35\gamma_{12}$. Due to being a noble metal and its efficiency as a plasmonic material resulting from the high plasma frequency, a spherical silver nanoparticle of a high-frequency dielectric constant of $\epsilon_{\infty}^{M} = 5$, plasmon energy of 9 e V and plasmon damping of $\gamma_M = 100\,\mathrm{TH_Z}$ is inserted in the system [50]. Note that, we apply a control field with a relatively low intensity corresponding to $1\,\mathrm{MH_Z}$ i.e. $58\,\mathrm{mW/m^2}$. To practically facilitate the setup, the inclination angles of the two plasmonic components with respect to the QD (θ_M, θ_G) are chosen to be equal and relatively large i.e. $\theta_M = \theta_G = 1$ rad.

In the following, we study the nonlinear absorption coefficients of the GND-MNP-QD hybrid system experienced by the probe field due to applying the control field. The effect of the edge-to-edge distances between GND and MNP (R) is examined in Fig. 2. Although we use low light intensity, the system exhibits giant cross-Kerr nonlinearity, compared to other nonlinear systems, can be controlled in magnitude and sign by the parameters of the system [45, 51]. In particular, the plasmonic system demonstrates large absorption coefficients that can be significantly controlled by the distances between the two plasmonic components. As the two plasmonic components come close to each other, the proposed plasmonic system exhibits large nonlinear absorption coefficients at exact resonance due to the corresponding strong dipole-dipole interaction between the components of the system. Obviously, the sign of the nonlinear absorption coefficient can be controlled by the probe field detuning. Moreover, it can be seen that the negative proportion of nonlinear absorption coefficient increases for small distances between the two plasmonic components implying the efficiency of the MNP-GND-QD hybrid system in nonlinear applications that require a switching between amplification and absorption. In fact, it is well-known that the coupling of plasmons is highly distance-dependent which stimulates many studies to suggest experimental techniques to control these distances such as nanolithography and related techniques [52, 53] that are limited in creating very small and well-defined inter-nanoparticle distances of few nanometers. Moreover, polymers and biomolecules can be used as spacers to tune the inter-nanoparticle distances of colloidal nanoparticles [54]. Therefore, the possibility to control the distances between plasmonic particles of the system provides an interesting property to control plasmonic photovoltaic devices.

Recently, it has been shown that the presence of MNP within the hybrid system can significantly improve the energy transfer between GND and QD [46]. Thus, the effect of the MNP size on nonlinear absorption coefficients is explored in Fig. 3. We observe that the nonlinear absorption

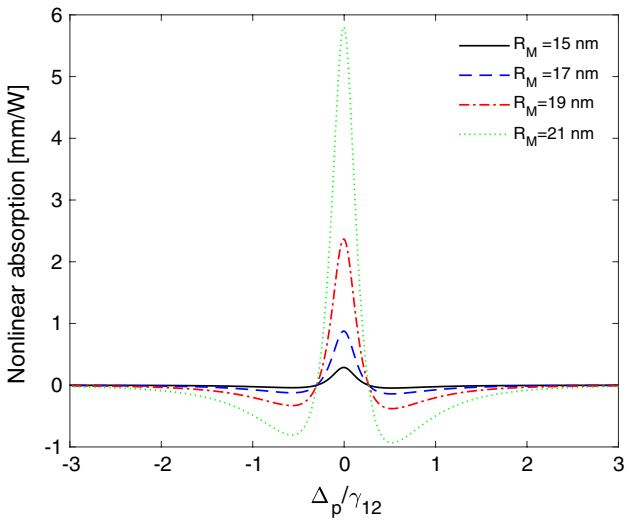

Fig. 3 Nonlinear absorption coefficient versus probe field detuning of the MNP-GND-QD hybrid system of geometry $\theta_M = \theta_G = 1$ rad, $R = 30\,\mathrm{nm}$, for different values of R_M. The system interacts with the resonant control field of $\Omega_c = 1\mathrm{MH_Z}$ and the probe field of $\Omega_p = 0.01\Omega_c$

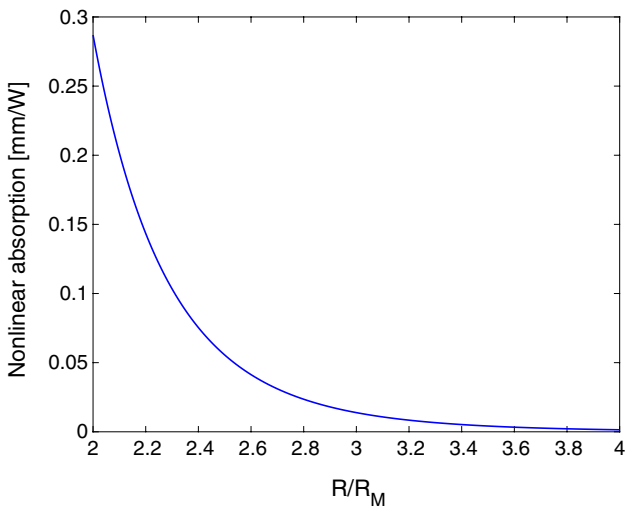

Fig. 4 Nonlinear absorption coefficient versus the ratio R/R_M of the MNP-GND-QD hybrid system of geometry $\theta_M = \theta_G = 1$ rad. The system interacts with the resonant control field of $\Omega_c = 1\,\mathrm{MH_Z}$ and the probe field of $\Omega_p = 0.01\Omega_c$

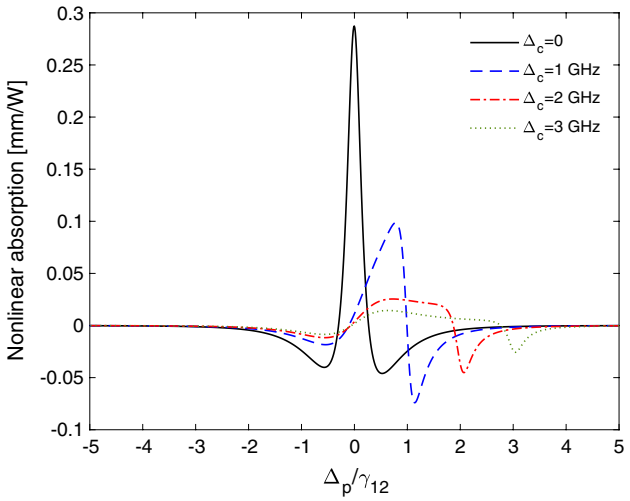

Fig. 5 Nonlinear absorption coefficient versus probe field detuning of the MNP-GND-QD hybrid system of geometry $\theta_M = \theta_G = 1$ rad, $R = 30$ nm and $R_M = 15$ nm, for different values of Δ_c. The system interacts with the resonant control field of $\Omega_c = 1\,\mathrm{MH_Z}$ and the probe field of $\Omega_p = 0.01\Omega_c$

coefficient is sensitive to the size of MNP. In particular, for relatively large size of the MNP, the nonlinear absorption of the system is significantly enhanced. Additionally, the sign of the nonlinear absorption coefficient can be controlled by the detuning of the probe field in addition to the size of the MNP providing a promising platform for many optical devices. To get a complete picture of the impact of both the edge-to-edge distances between the MNP and the GND (R) as well as the radius of the MNP (R_M), we study in Fig. 4 the behavior of the relation between the nonlinear absorption coefficient and the ratio R/R_M. Remarkably, the maximum values of the nonlinear absorption coefficients are obtained for a small R/R_M, when the separation between the MNP and GND is double the radius of the MNP. As the ratio R/R_M increases the nonlinear absorption coefficient significantly decreases. For $R/R_M > 3.5$, the nonlinear absorption coefficient vanishes as illustrated in Fig. 4.

Furthermore, due to the important role of the control field in the nonlinearity of the system via inducing the cross-Kerr effect, we examine the impact of the detuning of the control field on the nonlinear absorption coefficients in Fig. 5. Obviously, for resonant control field, we obtain a relatively large value of nonlinear absorption. As the ratio Δ_c/γ_{12} increases, the nonlinear absorption coefficients are significantly reduced and the peaks of the nonlinear absorption spectra are displaced to larger values along a wider band of the probe field detuning. Remarkably, the sign of the nonlinear absorption coefficients can be monitored by the detuning of the control field in addition to the detuning of the probe field.

Since the stability of the nonlinear system is a fundamental requirement for its significance in real-world applications, we check in Fig. 6 the behavior of the nonlinear absorption coefficients under the influence of a small

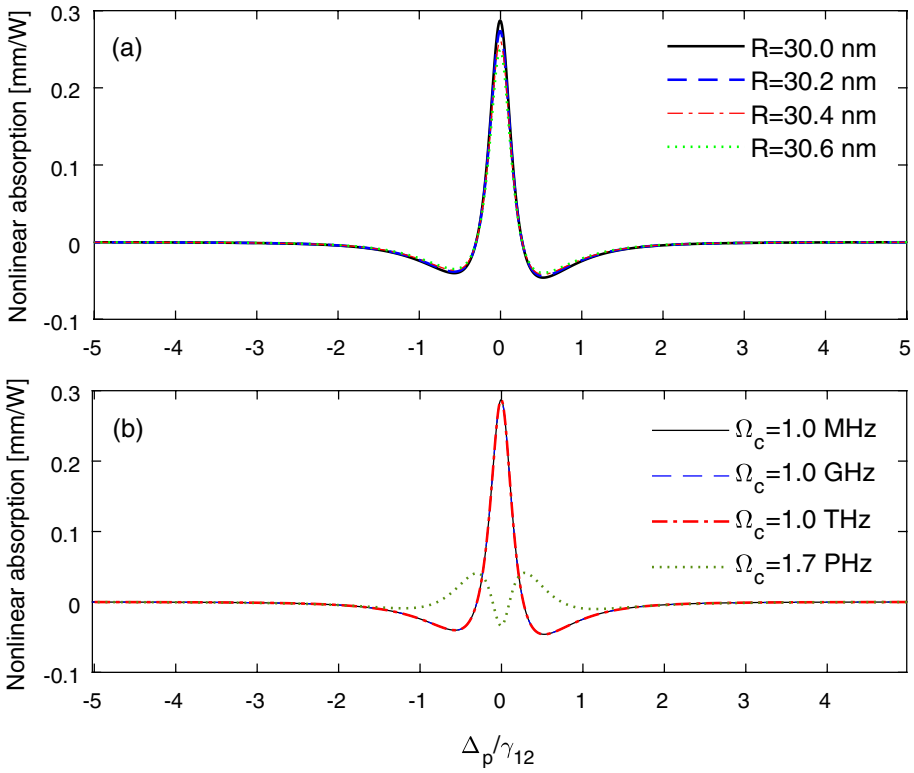

Fig. 6 Nonlinear absorption coefficient versus probe field detuning of the MNP-GND-QD hybrid system of geometry $\theta_M = \theta_G = 1$ rad, $R_M = 15$ nm and $R = 30$ nm (**b**). The system interacts with the control field of $\Omega_c = 1\,\mathrm{MH_Z}$ (**a**) and the probe field of $\Omega_p = 0.01\Omega_c$

variation of the geometrical parameters, i.e. the edge-to-edge distances between the GND and the MNP as well as the strength of the control field. Obviously, the nonlinear absorption of the system experiences a slight change as a result of small variations of its geometrical parameters despite the strong nonlinearity demonstrated by the system. Moreover, the system exhibits a good stability against considerable changes in the strength of the control field. When the control field becomes strong enough to induce electromagnetically induced transparency (EIT) i.e. 1.7 PHz, the nonlinear absorption coefficient is reduced associated with EIT window at exact resonance as shown in Fig. 6.

To conclude, from the above results, it is clear that the MNP-GND-QD hybrid system exhibits giant cross-Kerr nonlinearity compared to other plasmonic systems [44, 45]. Remarkably, the presence of the QD near the two plasmonic components, GND and MNP, can significantly enhance its cross-Kerr nonlinearity. This result can be attributed to the electric field enhancement in the MNP-GND-QD hybrid system recognized from the equation of motion for the density matrix elements Eq. 1, where the Rabi frequency of the electric field is enhanced by the factor $(\Pi_{x,z} + \Phi_{x,z})$ resulting from the dipole-dipole interaction between the components of the system. The obtained controllable large nonlinear absorption coefficients in the visible region of the electromagnetic spectrum associated with good stability emphasizes the importance of the system for constructing efficient photovoltaic devices with limited losses and high efficiency due to the low light intensity required to demonstrates this giant cross-Kerr nonlinearity.

4 Conclusion

We have studied the cross-Kerr of the MNP-GND-QD hybrid system experienced by the probe field due to the presence of another control field. We have derived an analytical expression for the third-order nonlinear susceptibility of cross-Kerr nonlinearity. A giant cross-Kerr nonlinearity is obtained that can be controlled by the geometrical features of the system in addition to the detuning of both probe and control fields. Interestingly, the system exhibits large nonlinear absorption coefficients in the visible region of the electromagnetic spectrum with low light intensity for small distances between the MNP and the GND and large size of the MNP as well as the small detuning of the control field. Specifically, large values of cross-Kerr nonlinear absorption coefficient are obtained for a resonant control field with a ratio of the separation between GND and MNP to the size of MNP is equal to 2. Moreover, a controllable switching between positive and negative nonlinear absorption is observed that implies the possibility of using the MNP-GND-QD hybrid system in various applications that require amplification and absorption.

The large nonlinear absorption coefficients with good stability in the visible region of the electromagnetic spectrum demonstrated by our proposed plasmonic system emphasizes that the system can provide a promising platform for photovoltaic devices. We hope that our study will stimulate more efforts to experimentally examine the nonlinear properties of our proposed MNP-GND-QD hybrid system and its potential applications.

Acknowledgements The authors extend their appreciation to the Deanship of Scientific Research at King Khalid University for funding this work through General Research Project under grant number (GRP/73/43).

References

1. K. Rottwitt, P. Tidemand-Lichtenberg, *Nonlinear optics: principles and applications*, vol. 3 (CRC Press, Boca Raton, 2014)
2. P.S. Kuo, M. Fejer, Mixing of polarization states in zincblende nonlinear optical crystals. Opt. Express **26**(21), 26971–26984 (2018)
3. M. Kauranen, A.V. Zayats, Nonlinear plasmonics. Nat. Photon. **6**(11), 737–748 (2012)
4. B. Jin, C. Argyropoulos, Enhanced four-wave mixing with nonlinear plasmonic metasurfaces. Sci. Rep. **6**(1), 1–9 (2016)
5. M.M. Tohari, A. Lyras, M.S. AlSalhi, Giant self-kerr nonlinearity in the metal nanoparticles-graphene nanodisks-quantum dots hybrid systems under low-intensity light irradiance. Nanomaterials **8**(7), 521 (2018)
6. Z. Ziani, G. Lévêque, A. Akjouj, S. Coulibaly, A. Taki, Characterization of spatiotemporal chaos in arrays of nonlinear plasmonic nanoparticles. Phys. Rev. B **100**(16), 165423 (2019)
7. A.V. Zayats, I.I. Smolyaninov, A.A. Maradudin, Nano-optics of surface plasmon polaritons. Phys. Rep. **408**(3–4), 131–314 (2005)
8. P.V. Kamat, G.V. Hartland, Plasmons for energy conversion. ACS Energy Lett. **3**(6), 1467–1469 (2018)
9. W. Ye, R. Long, H. Huang, Y. Xiong, Plasmonic nanostructures in solar energy conversion. J. Mater. Chem. C **5**(5), 1008–1021 (2017)
10. S. Sadeghi, Gain without inversion in hybrid quantum dot-metallic nanoparticle systems. Nanotechnology **21**(45), 455401 (2010)
11. B. Tang, L. Dai, C. Jiang, Electromagnetically induced transparency in hybrid plasmonic-dielectric system. Opt. express **19**(2), 628–637 (2011)
12. S.G. Kosionis, A.F. Terzis, S.M. Sadeghi, E. Paspalakis, Optical response of a quantum dot-metal nanoparticle hybrid interacting with a weak probe field. J. Phys. Conden. Matter **25**(4), 045304 (2012)
13. S. Evangelou, V. Yannopapas, E. Paspalakis, Transparency and slow light in a four-level quantum system near a plasmonic nanostructure. Phys. Rev. A **86**(5), 053811 (2012)
14. F. Carreño, M. Antón, V. Yannopapas, E. Paspalakis, Control of the absorption of a four-level quantum system near a plasmonic nanostructure. Phys. Rev. B **95**(19), 195410 (2017)
15. G. Solookinejad, Surface plasmon assisted superluminal light propagation in a quantum dot-metallic nanoparticle hybrid system. Laser Phys. **28**(10), 105201 (2018)

16. H.-J. Chen, Fano resonance induced fast to slow light in a hybrid semiconductor quantum dot and metal nanoparticle system. Laser Phys. Lett. **17**(2), 025201 (2020)
17. K.R. Catchpole, S. Mokkapati, F. Beck, E.-C. Wang, A. McKinley, A. Basch, J. Lee, Plasmonics and nanophotonics for photovoltaics. Mrs Bull. **36**(6), 461–467 (2011)
18. H.A. Atwater, A. Polman, Plasmonics for improved photovoltaic devices. In: *Materials for sustainable energy: a collection of peer-reviewed research and review articles from Nature Publishing Group*, 1–11 (2011)
19. S. Pillai, M. Green, Plasmonics for photovoltaic applications. Solar Energy Mater. Solar Cells **94**(9), 1481–1486 (2010)
20. E. Stratakis, E. Kymakis, Nanoparticle-based plasmonic organic photovoltaic devices. Mater. Today **16**(4), 133–146 (2013)
21. N.-W. Teng, S.-S. Yang, F.-C. Chen, Plasmonic-enhanced organic photovoltaic devices for low-power light applications. IEEE J. Photovolt. **8**(3), 752–756 (2018)
22. W.-J. Ho, S.-K. Feng, J.-J. Liu, Y.-C. Yang, C.-H. Ho, Improving photovoltaic performance of silicon solar cells using a combination of plasmonic and luminescent downshifting effects. Appl. Surface Sci. **439**, 868–875 (2018)
23. S. Fathpour, K.K. Tsia, B. Jalali, Nonlinear photovoltaic effect. In: *LEOS 2007-IEEE Lasers and Electro-Optics Society Annual Meeting Conference Proceedings*, pp. 892–893 (2007). IEEE
24. R. Sebastian, S. Sankararaman, Development and nonlinear optical characterization of phthalocyanine-incorporated stable natural dye with wideband absorption for solar cell applications. JOSA B **37**(1), 110–116 (2020)
25. A.M. Abu Baker, G.S. Boltaev, M. Iqbal, M. Pylnev, N.M. Hamdan, A.S. Alnaser, Giant third-order nonlinear response of mixed perovskite nanocrystals. Materials **15**(1), 389 (2022)
26. J.B. Khurgin, G. Sun, Plasmonic enhancement of the third order nonlinear optical phenomena: figures of merit. Opt. Express **21**(22), 27460–27480 (2013)
27. E. Paspalakis, S. Evangelou, S.G. Kosionis, A.F. Terzis, Strongly modified four-wave mixing in a coupled semiconductor quantum dot-metal nanoparticle system. J. Appl. Phys. **115**(8), 083106 (2014)
28. A. Terzis, S. Kosionis, J. Boviatsis, E. Paspalakis, Nonlinear optical susceptibilities of semiconductor quantum dot-metal nanoparticle hybrids. J. Mod. Opt. **63**(5), 451–461 (2016)
29. R.W. Boyd, *Nonlinear optics* (Academic press, Cambridge, 2020)
30. S. Rebić, D. Vitali, C. Ottaviani, P. Tombesi, M. Artoni, F. Cataliotti, R. Corbalán, Polarization phase gate with a tripod atomic system. Phys. Rev. A **70**(3), 032317 (2004)
31. C. Zhu, G. Huang, Giant kerr nonlinearity, controlled entangled photons and polarization phase gates in coupled quantum-well structures. Opt. Express **19**(23), 23364–23376 (2011)
32. S. Zhang, F. Zang, L. Dong, L. Li, The evolution and interaction of the asymmetric pearcey-gaussian beam in nonlinear kerr medium. Appl. Phys. B **128**(9), 1–9 (2022)
33. H. Schmidt, A. Imamoglu, Giant kerr nonlinearities obtained by electromagnetically induced transparency. Opt. Lett. **21**(23), 1936–1938 (1996)
34. H. Kang, Y. Zhu, Observation of large kerr nonlinearity at low light intensities. Phys. Rev. Lett. **91**(9), 093601 (2003)
35. H. Sun, Y. Niu, S. Jin, S. Gong, Phase control of cross-phase modulation with electromagnetically induced transparency. J. Phys. B: Atom. Mol. Opt. Phys. **40**(15), 3037 (2007)
36. J. Kou, R. Wan, Z. Kang, H. Wang, L. Jiang, X. Zhang, Y. Jiang, J. Gao, Eit-assisted large cross-kerr nonlinearity in a four-level inverted-y atomic system. JOSA B **27**(10), 2035–2039 (2010)
37. X. Yang, S. Li, C. Zhang, H. Wang, Enhanced cross-kerr nonlinearity via electromagnetically induced transparency in a four-level tripod atomic system. JOSA B **26**(7), 1423–1434 (2009)
38. L. Wang, X. Yan, Effective cross-kerr effect in the n-type four-level atom. In: Electronics and Signal Processing, pp. 421–426. Springer (2011)
39. B. Behroozian, H. Askari, Kerr nonlinearity and nonlinear absorption coefficient in a four-level m-model cylindrical quantum dot under the phenomenon of electromagnetically induced transparency. Laser Phys. **28**(7), 075401 (2018)
40. L.V. Doai, Giant cross-kerr nonlinearity in a six-level inhomogeneously broadened atomic medium. J. Phys. B Atom. Mol. Phys. **52**(22), 225501 (2019)
41. N.L.T. An, D.X. Khoa, V.N. Sau, N.H. Bang et al., Manipulating giant cross-kerr nonlinearity at multiple frequencies in an atomic gaseous medium. JOSA B **36**(10), 2856–2862 (2019)
42. M. El barghouti, O. Haidar, A. Akjouj, A. Mir, Figure of merit and sensitivity enhancement of biosensor lspr in investigated for visible and near infrared. Photon. Nanostruct. Fund. Appl. **50**, 101016 (2022)
43. C. Torres-Torres, B. Can-Uc, R. Rangel-Rojo, L. Castañeda, R. Torres-Martinez, C. García-Gil, A. Khomenko, Optical kerr phase shift in a nanostructured nickel-doped zinc oxide thin solid film. Opt. Express **21**(18), 21357–21364 (2013)
44. H. Rahman, H. Bibi, M.A. Jabar, I. Ahmad, Cross-kerr nonlinearity in the surface plasmon polariton waves generated at the interface of graphene and gain medium. EPL (Europhys. Lett.) **122**(5), 57003 (2018)
45. M. Javanmard, High refractive index and enhanced cross-kerr nonlinearity in five-level quantum systems near plasmonic structure. Braz. J. Phys. **51**(6), 1509–1520 (2021)
46. M. Tohari, A. Lyras, M. Alsalhi, Ultrafast energy transfer in the metal nanoparticles-graphene nanodisks-quantum dots hybrid systems. Plasmonics **14**(1), 17–24 (2019)
47. M.M. Tohari, M.M. Alqahtani, A. Lyras, Optical multistability in the metal nanoparticle-graphene nanodisk-quantum dot hybrid systems. Nanomaterials **10**(9), 1687 (2020)
48. M.M. Tohari, Terahertz optical bistability in the metal nanoparticles-graphene nanodisks-quantum dots hybrid systems. Nanomaterials **10**(11), 2173 (2020)
49. S. Thongrattanasiri, A. Manjavacas, F.J. García de Abajo, Quantum finite-size effects in graphene plasmons. Acs Nano **6**(2), 1766–1775 (2012)
50. S.V. Gaponenko, *Introduction to nanophotonics* (Cambridge University Press, Cambridge, 2010)
51. Z. Lu, K.-D. Zhu, Enhancing kerr nonlinearity of a strongly coupled exciton-plasmon in hybrid nanocrystal molecules. J. Phys. B: Atom. Mol. Opt. Phys. **41**(18), 185503 (2008)
52. A. Kinkhabwala, Z. Yu, S. Fan, Y. Avlasevich, K. Müllen, W.E. Moerner, Large single-molecule fluorescence enhancements produced by a bowtie nanoantenna. Nat. Photon. **3**(11), 654–657 (2009)
53. A. Bek, R. Jansen, M. Ringler, S. Mayilo, T.A. Klar, J. Feldmann, Fluorescence enhancement in hot spots of afm-designed gold nanoparticle sandwiches. Nano Lett. **8**(2), 485–490 (2008)
54. X. Yu, D.Y. Lei, F. Amin, R. Hartmann, G.P. Acuna, A. Guerrero-Martínez, S.A. Maier, P. Tinnefeld, S. Carregal-Romero, W.J. Parak, Distance control in-between plasmonic nanoparticles via biological and polymeric spacers. Nano Today **8**(5), 480–493 (2013)